

Single-inclusive hadron production in electron-positron annihilation at next-to-next-to-next-to-leading order in QCD

Chuan-Qi He ^{1,2,3,*} Hongxi Xing ^{1,2,4,†} Tong-Zhi Yang ^{5,‡} and Hua Xing Zhu ^{6,7,§}

¹*State Key Laboratory of Nuclear Physics and Technology, Institute of Quantum Matter, South China Normal University, Guangzhou 510006, China*

²*Guangdong Basic Research Center of Excellence for Structure and Fundamental Interactions of Matter, Guangdong Provincial Key Laboratory of Nuclear Science, Guangzhou 510006, China*

³*Key Laboratory of Atomic and Subatomic Structure and Quantum Control (MOE), Guangdong-Hong Kong Joint Laboratory of Quantum Matter, Guangzhou 510006, China*

⁴*Southern Center for Nuclear-Science Theory (SCNT), Institute of Modern Physics, Chinese Academy of Sciences, Huizhou 516000, China*

⁵*Physik-Institut, Universität Zürich, Winterthurerstrasse 190, 8057 Zürich, Switzerland*

⁶*School of Physics, Peking University, Beijing 100871, China*

⁷*Center for High Energy Physics, Peking University, Beijing 100871, China*

Single-inclusive hadron production in electron-positron annihilation (SIA) represents the cleanest process for investigating the dynamics of parton hadronization, as encapsulated in parton fragmentation functions. In this letter, we present, for the first time, the analytical computation of Quantum Chromodynamics (QCD) corrections to the coefficient functions for SIA at next-to-next-to-next-to-leading order (N³LO) accuracy, achieving the highest precision to date for hadron production processes. Utilizing the BaBar measurement as a benchmark, we assess the phenomenological implications of this high-precision calculation. Our findings demonstrate a substantial reduction in scale uncertainties at N³LO and offer an improved description of the experimental data compared to lower-order calculations. This advancement underscores the importance of higher-order corrections in achieving a more accurate understanding of hadronization processes.

Introduction. – The investigation of hadron production in high-energy particle collisions, such as electron-positron, electron-proton, and proton-proton scatterings, offers profound insights into the non-perturbative dynamics of Quantum Chromodynamics (QCD) [1]. Among these processes, single-inclusive hadron production in electron-positron annihilation (SIA) is particularly significant, as it represents the cleanest and most direct probe of parton hadronization. This hadronization process is quantitatively described by parton fragmentation functions (FFs) [2–4], which encapsulate the probability distributions for quarks and gluons to transition into observable hadrons. FFs are indispensable tools for unraveling the structure of matter and elucidating the intricate dynamics of QCD at low energy scales, making them a fundamental quantity of modern particle physics research [5, 6].

Precision calculations of partonic coefficient functions for hadron production in perturbative QCD (pQCD) are crucial for extracting reliable information about the fundamental QCD properties, such as FFs [5] and the strong coupling constant [7], from experimental data. These coefficient functions have been computed up to next-to-next-to-leading order (NNLO) for SIA [8, 9], and more recently for electron-proton [10–14] and proton-proton collisions [15]. Progress has also been made toward the NNLO computation of fiducial cross sections with identified hadrons [15–17]. These results, together with the NNLO time-like splitting functions [18–21] has enabled global analyses of fragmentation functions (FFs) at NNLO accuracy [22–28]. These advances underscore the critical synergy between fixed-order NNLO calcula-

tions and global QCD analyses.

NNLO calculations have already led to substantial improvements in reducing theoretical uncertainties and enhancing agreement with experimental measurements. However, given the precision of modern SIA datasets (e.g., BaBar, Belle, LEP, BESIII) and the proposed future lepton colliders, such as the CEPC [29–31], STCF [32], ILC [33–35], and FCC-*ee* [36–38], theoretical uncertainties now risk limiting the statistical power of global FF analyses. Achieving N³LO accuracy for SIA is therefore essential to further constrain parton fragmentation functions and advance our understanding of hadronization dynamics.

In this letter, we present a significant advancement in this direction: we extend the analytic continuation in Ref. [18] to the scattering process in full QCD and, for the first time, obtain the complete results for SIA coefficient functions at N³LO accuracy. To assess the phenomenological impact of our results, we compare our N³LO predictions with the BaBar measurement, a benchmark dataset in the study of SIA. Our findings reveal a substantial reduction in scale uncertainties at N³LO and demonstrate an improved description of the experimental data compared to lower-order calculations. By providing a more accurate and reliable description of parton hadronization, our results contribute to a deeper understanding of the strong interaction.

Kinematics of SIA. – We focus on the photon exchange process of SIA in e^+e^- collisions

$$e^+ + e^- \rightarrow \gamma^*(q) \rightarrow h(p) + X, \quad (1)$$

where q and p represent the four-momenta of the virtual photon and the identified hadron h , respectively, X denotes any inclusive final hadronic state. In this process, the unpolarized differential cross section can be written as [39, 40]

$$\frac{d^2\sigma^h}{dx d\cos\theta} = \frac{3}{8}(1 + \cos^2\theta) \frac{d\sigma_T^h}{dx} + \frac{3}{4}\sin^2\theta \frac{d\sigma_L^h}{dx}, \quad (2)$$

where the variable θ denotes the angle of h with respect to the electron beam direction in the center of mass frame. The Bjorken variable is defined as $x = 2p \cdot q/Q^2$ with $Q^2 = q^2$. According to the leading twist QCD factorization, the transverse (T) and longitudinal (L) differential cross sections can be factorized into the following form:

$$\frac{d\sigma_k^h}{dx} = \sum_q \sum_j (D_j^h \otimes C_{jq} + D_j^h \otimes C_{j\bar{q}})(x) \times \sigma_{q\bar{q}}^{(0)}, \quad (3)$$

where $k = T, L$, and we omit the index k in the coefficient function C . $\sigma_{q\bar{q}}^{(0)} = \frac{4\pi\alpha_e^2}{3Q^2} N_c e_q^2$ is the born-level cross section. The convolution is defined as $(D \otimes C)(x) = \int_x^1 \frac{dz}{z} D(z) C(x/z)$. In Eq. (3), D_j^h is parton fragmentation functions, representing the probability density of parton j fragmenting into hadron h , and j runs over all parton flavors including gluon. Using charge conjugation invariance of the strong interactions, we have $C_{qq} = C_{\bar{q}\bar{q}}$, $C_{\bar{q}q} = C_{q\bar{q}}$, $C_{gq} = C_{g\bar{q}}$. Then Eq. (3) can be reorganized into the following form,

$$\begin{aligned} \frac{d\sigma_k^h}{dx} = & D_g^h \otimes (2C_{gq}) \sum_{q=1}^{N_f} \sigma_{q\bar{q}}^{(0)} \\ & + \sum_{q=1}^{N_f} (D_q^h + D_{\bar{q}}^h) \otimes (C_{qq}^V + C_{q\bar{q}}^V) \sigma_{q\bar{q}}^{(0)} \\ & + \sum_{q'=1}^{N_f} (D_{q'}^h + D_{\bar{q}'}^h) \otimes (C_{q'q} + C_{q'\bar{q}}) \sum_{q=1}^{N_f} \sigma_{q\bar{q}}^{(0)}, \end{aligned} \quad (4)$$

where N_f is the number of massless quark flavors, and the valence coefficient functions are defined by $C_{qq}^V = C_{qq} - C_{q'q}$, $C_{q\bar{q}}^V = C_{q\bar{q}} - C_{q'\bar{q}}$. In this letter, we determine the N³LO corrections, i.e. the coefficient of a_s^3 with $a_s = \alpha_s/(4\pi)$, to the partonic coefficient functions C_{gq} , $C_{qq}^V + C_{q\bar{q}}^V$, $C_{q'q} + C_{q'\bar{q}}$ in Eq. (4), and we work in dimensional regularization with the dimension $d = 4 - 2\epsilon$.

The method.— At N³LO, one, in principle, needs to compute the contributions from all relevant cuts, i.e., triple real (RRR), double-real virtual (VRR), double-virtual real (VVR), virtual-squared real (VV*R) and triple virtual (VVV). Some sample Feynman diagrams are shown in Fig. 1. Although the contribution from VVV has been known for over a decade [41], the real corrections are significantly more complex and have never been evaluated, preventing the extraction of SIA at N³LO.

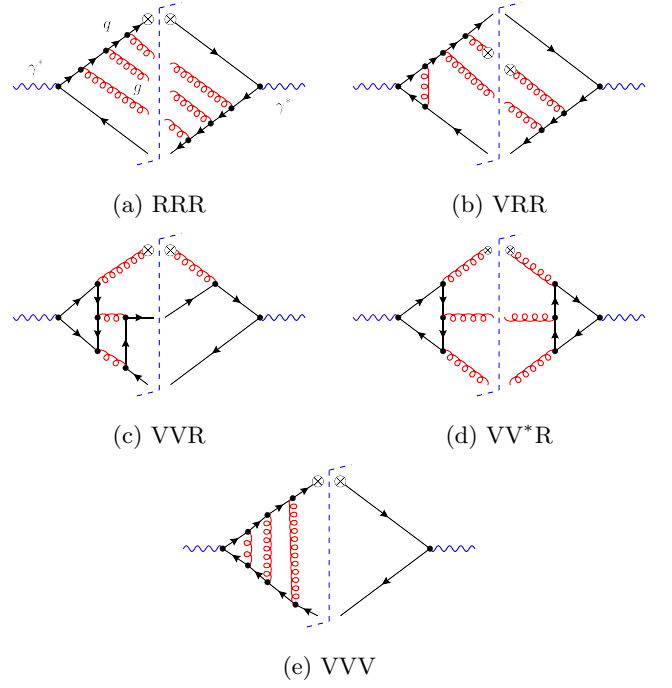


FIG. 1: Sample cut Feynman diagrams contributing to SIA coefficient functions, where the crossed bubble represents a single identified parton.

Fortunately, an exploration of analytic continuation from deep inelastic scattering (DIS) could significantly simplify the computations for SIA. At LO, the partonic channel for DIS reads $\gamma^*(q) + \text{quark}(p) \rightarrow \text{quark}(k)$, where the corresponding Bjorken variable in space-like region is $x_B = -q^2/(2p \cdot q)$ with $q^2 < 0$. While for SIA, the corresponding partonic channel reads $\gamma^*(q) \rightarrow \text{anti-quark}(p) + \text{quark}(k)$, where $x = 2p \cdot q/q^2$ with $q^2 > 0$. These two processes are related by crossing symmetry, i.e., SIA can be obtained from DIS by replacing an incoming quark with an outgoing anti-quark. In terms of momenta and Bjorken variables, the analytic continuation rule reads

$$p \rightarrow -p, \quad x_B = \frac{-q^2}{2p \cdot q} \rightarrow \frac{-q^2}{-2p \cdot q} = \frac{1}{x}. \quad (5)$$

The above rule has been noted long ago in Refs. [42, 43]. However, a direct analytic continuation for cross-section-level quantities fails beyond two-loop order [19–21, 44]. This problem has been carefully analyzed and resolved in Ref. [18] within the context of analytic continuation for transverse-momentum-dependent beam and fragmentation functions at N³LO. We extend this method to scattering processes in full QCD and further address the previously unconsidered analytic continuation for the VV*R contribution. The issue stems from the fact that analytic continuation should be performed at the bare amplitude level, i.e., before summing over the corresponding com-

plex conjugate contributions, rather than at the renormalized cross-section level.

The analytic continuation rule $x_B \rightarrow 1/x$ only crosses the branch cut $x_B = x = 1$. Therefore, it is sufficient to analyze the threshold limits for all different cut contributions at the bare amplitude level. Tab. I and Tab. II show the structures in the threshold limit for DIS and SIA, respectively. In the tables, the results are organized to factor out an overall factor $[(p+q)^2]^{-3\epsilon}$ for DIS and $[(-p+q)^2]^{-3\epsilon}$ for SIA. The first factor gives rise to the prescription for x_B , i.e. $(p+q)^2 + i0^+$ gives $x_B = \text{Re}[x_B] - i0^+$, where “Re” denotes the real part. These two factors are real in their respective regions and are related by the crossing rule $p \rightarrow -p$, such

that the remaining parts are related to each other by $1 - x_B \rightarrow (1/x - 1)e^{i\pi}$ [18]. Special attention is required for the analytic continuation of the VV*R contribution, since it simultaneously involves V and its complex conjugate. To this end, we carefully track the contributions from V and V* by using x_B and its complex conjugate x_B^* , respectively. Here, x_B and x_B^* are $x_B = \text{Re}[x_B] - i0^+$ and $x_B^* = \text{Re}[x_B] + i0^+$. The analytic continuation rule for x_B^* then reads $1 - x_B^* \rightarrow (1/x^* - 1)e^{-i\pi}$. As a brief summary, the analytic continuation rule in Eq. (5) is modified to

$$\begin{aligned} p &\rightarrow -p, & 1 - x_B &= (1/x - 1)e^{i\pi}, \\ 1 - x_B^* &\rightarrow (1/x^* - 1)e^{-i\pi}. \end{aligned} \quad (6)$$

Cuts	Threshold-limit structures for DIS
RRR	$[(p+q)^2]^{-3\epsilon} B_0$
VRR	$[(p+q)^2]^{-3\epsilon} [B_s e^{i\pi\epsilon} + B_c (1 - x_B)^\epsilon]$
VVR	$[(p+q)^2]^{-3\epsilon} [B_{s,s} e^{2i\pi\epsilon} + B_{s,c} e^{i\pi\epsilon} (1 - x_B)^\epsilon + B_{c,c} (1 - x_B)^{2\epsilon}]$
VV*R	$[(p+q)^2]^{-3\epsilon} [B_{s,s} + B_{c,s} e^{i\pi\epsilon} (1 - x_B^*)^\epsilon + B_{c,s} e^{-i\pi\epsilon} (1 - x_B)^\epsilon + B_{c,c} (1 - x_B)^\epsilon (1 - x_B^*)^\epsilon]$

TABLE I: The structures of the DIS coefficient function for different cuts in the threshold limit at N³LO, where the coefficients $B_0, B_s, B_{c,s}, \dots$ are purely real, and x_B^* is the complex conjugate of x_B .

Cuts	Threshold-limit structures for SIA
RRR	$[(-p+q)^2]^{-3\epsilon} F_0$
VRR	$[(-p+q)^2]^{-3\epsilon} e^{i\pi\epsilon} [F_s + F_c (1 - x)^\epsilon]$
VVR	$[(-p+q)^2]^{-3\epsilon} e^{2i\pi\epsilon} [F_{s,s} + F_{s,c} (1 - x)^\epsilon + F_{c,c} (1 - x)^{2\epsilon}]$
VV*R	$[(-p+q)^2]^{-3\epsilon} [F_{s,s} + F_{c,s} (1 - x^*)^\epsilon + F_{c,s} (1 - x)^\epsilon + F_{c,c} (1 - x)^\epsilon (1 - x^*)^\epsilon]$

TABLE II: The structures of SIA coefficient function for different cuts in the threshold limit at N³LO, where the coefficients $F_0, F_s, F_{c,s}, \dots$ are purely real, and x^* is the complex conjugate of x .

The currently known coefficient functions for DIS at N³LO [45] are computed from forward scattering, i.e., they are the summation of all cut contributions and their complex conjugates. Tab. I shows that the summation of the RRR, VRR, and their complex conjugate contributions still produces correct results under a direct analytic continuation, up to a purely imaginary part. However, this is not the case for VVR and VV*R. Explicitly,

$$\begin{aligned} &[\mathcal{AC}(\text{VVR}) + \text{c.c.}] - \text{Re}[\mathcal{AC}(\text{VVR} + \text{c.c.})] \\ &\propto B_{s,c} \sin^2(\pi\epsilon) \neq 0, \\ &\mathcal{AC}(\text{VV}^*\text{R}) - \text{Re}[\mathcal{AC}(\text{VV}^*\text{R}|_{x_B^* \rightarrow x_B})] \\ &\propto [B_{c,c} + B_{c,s}] \sin^2(\pi\epsilon) \neq 0, \end{aligned} \quad (7)$$

where \mathcal{AC} and c.c. denote analytic continuation based on the rule in Eq. (6) and complex conjugate, respec-

tively. The $\mathcal{AC}(\text{VV}^*\text{R}|_{x_B^* \rightarrow x_B})$ represents the direct analytic continuation of the cross-section-level quantity for VV*R. Unlike the cases of RRR and VRR, the above differences are non-zero and contribute to finite part when multiplying with an ϵ -divergent coefficient.

To maximally reduce the complexity of computations, we propose the following analytic continuation formula for the N³LO correction, schematically:

$$\begin{aligned} d\sigma^{(3), \text{SIA}} &= \text{Re} \left[\mathcal{AC} \left(d\sigma^{(3), \text{DIS}} \right) \right. \\ &\quad - \mathcal{AC} \left(d\sigma_{\text{VVR}}^{(3), \text{DIS}} + \text{c.c.} \right) - \mathcal{AC} \left(d\sigma_{\text{VV}^*\text{R}}^{(3), \text{DIS}} \Big|_{x_B^* \rightarrow x_B} \right) \\ &\quad \left. + \left\{ \mathcal{AC} \left(d\sigma_{\text{VVR}}^{(3), \text{DIS}} \right) + \text{c.c.} \right\} + \mathcal{AC} \left(d\sigma_{\text{VV}^*\text{R}}^{(3), \text{DIS}} \right) \right]. \end{aligned} \quad (8)$$

We emphasize that each term above is understood as an unrenormalized quantity. The first term represents a direct analytic continuation of the differential cross section at N³LO for DIS [45], which includes problematic contributions from VVR and VV*R. In the second line, the problematic contributions are subtracted, and in the third line, the contributions from the correct analytic continuation are restored. Therefore, to obtain the coefficient functions for SIA at N³LO, we need to explicitly compute the VVR and VV*R contributions for DIS. Alternatively, we can compute the VVR and VV*R contributions directly for SIA and analytically continue them back to the DIS region. The VVR and VV*R contributions for both the DIS and SIA regions have not been reported in the literature. In the next section, we explicitly evaluate these contributions in the SIA region.

*Computations of VVR and VV*R.*— We use the following projectors to extract the transverse and longitudinal partonic coefficient functions [8, 9]

$$\begin{aligned} C_{T,p}(x, Q^2) &= \frac{1}{d-2} \left(-\frac{2p \cdot q}{q^2} g^{\mu\nu} - \frac{2}{p \cdot q} p^\mu p^\nu \right) \hat{W}_{\mu\nu}, \\ C_{L,p}(x, Q^2) &= \frac{1}{p \cdot q} p^\mu p^\nu \hat{W}_{\mu\nu}, \end{aligned} \quad (9)$$

where $\hat{W}_{\mu\nu}$ is the parton structure tensor defined by $\hat{W}_{\mu\nu}(p, q) = \frac{x^{1-2\epsilon}}{4\pi} \int d\text{PS}^{(l)} M_\mu^{\gamma^* \rightarrow p+X} (M_\nu^{\gamma^* \rightarrow p+X})^*$. Here, the factor $x^{1-2\epsilon}$ is from the phase-space of the single identified parton, $\int d\text{PS}^{(l)}$ is the l -body invariant phase space measure, and $M_\mu^{\gamma^* \rightarrow p+X}$ is the amplitude for process $\gamma^*(q) \rightarrow p + p_1 + p_2 + \dots + p_l$ with p and p_1, \dots, p_l being the momenta of the identified parton and unidentified partons, respectively.

Using the above projectors, the computations for VVR and VV*R follow the standard multi-loop techniques. We utilize **QGRAF** [46] to generate all relevant Feynman diagrams, and **Form** [47, 48], **Color** [49] to evaluate Dirac and color algebra. The method of reverse unitarity [50] is employed to enable the application of standard integration-by-parts (IBP) reductions [51–53] for mixed loop and phase-space integrals. In this work, we utilize **FIRE6** [54], **Kira** [55] and **Blade** [56] to reduce a large number of integrals to a basis of integrals, called *master integrals*. We identified all master integrals from 24 integral families for VVR and from 10 integral families for VV*R. We then directly solve these master integrals using the differential equation (DE) method [57], with the boundary constants determined by matching to inclusive integrals for VVR and VV*R [58, 59]. The DE system is derived with the aid of **LiteRed** [60], and converted into canonical form [61] by the package **CANONICA** [62]. It should be noted that, under analytic continuation, contributions from different branches at $x = 1$, i.e. $(1-x)^{a\epsilon}$ with a being integers, should be separated. Since different branches do not interact before expanding ϵ , it is straightforward to construct and solve the DEs for dif-

ferent branches independently.

The explicit bare result for VVR up to finite term in ϵ only involves letters $\{x, 1-x\}$, which can be expressed in term of harmonic polylogarithms (HPLs) [63]. On the other hand, the bare result for VV*R contains letters $\{x, 1-x, 2-x\}$ in finite term, which involves Goncharov multiple polylogarithms (GPLs). We use **HPL** [64] and **Polylogtools** [65] packages to deal with HPLs and GPLs, respectively.

Result.— In addition to the new bare results for VVR and VV*R, the lower-order results in a_s up to higher-order in ϵ and collinear counterterms are also necessary. We explicitly computed NNLO corrections up to $\mathcal{O}(\epsilon^2)$ for both DIS and SIA, which are not yet publicly available in the literature, and verified that the analytic continuation relation holds between them. The collinear counterterms for FFs are composed of NNLO time-like splitting functions [18–21]. Notice that the collinear counterterms for parton distribution functions (PDFs), which are composed of NNLO space-like splitting functions [66, 67], are also required to extract the bare results at N³LO for DIS from the renormalized ones [45]. By utilizing the analytic continuation formula in Eq. (8), and performing mass factorization using lower-order results and collinear counterterms, we managed to obtain the analytic results for SIA partonic coefficient functions at N³LO, except for $\delta(1-x)$ term. The analytic continuation of $\delta(1-x)$ term requires to track terms $(1-x_B)^{-1+a\epsilon}$ in all cut contributions as well as $\delta(1-x_B)$ term from the 3-loop form factor [41], which is quite involved. Instead, we determine the $\delta(1-x)$ contribution through sum rules, i.e., integrating over x and match with the inclusive cross section at N³LO [68, 69].

The final results for coefficient functions are expressed in terms of HPLs, and we have performed several consistency checks: First, all poles in ϵ cancel when using the three-loop time-like splitting functions [18–21]. Second, the $\delta(1-x)$ term is fully consistent with a recent result from threshold resummation at N⁴LL accuracy [70]. Third, by integrating over x in our explicit results for VVR and VV*R, we find complete agreement with the inclusive results in Ref. [71]. Fourth, the NNLO corrections are in full agreement with Refs. [8, 9]. The final results are too lengthy to be presented here, we have included them in an ancillary file submitted with this paper.

To assess the phenomenological impact of our results, we perform numerical calculations at N³LO. As a benchmark comparison, we confront our predictions with the high precision BaBar measurements at collision energy $\sqrt{s} = 10.54$ GeV [72]. Since FFs at N³LO accuracy are not yet available, we employ the NNFF1.0 [22] parametrization, which provides FFs from LO to NNLO accuracy, as a proxy to illustrate the impact of N³LO corrections. For the numerical evaluation of HPLs, we utilize the package **hplog** [73].

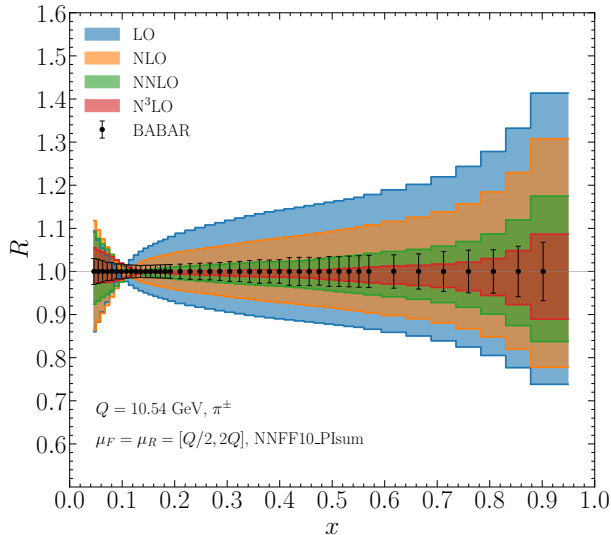


FIG. 2: The relative uncertainties with respect to the scale choice $\mu_F = \mu_R = Q$, arise from the variation of QCD scales at each pQCD orders represented by different color bands. The error bars indicate the uncertainty from BaBar measurements.

We first analyze the scale dependence of our results in Fig. 2, where the ratio R is defined as the relative uncertainty with respect to the QCD scale choice $\mu_F = \mu_R = Q$. The colored bands represent the scale uncertainties by varying the QCD scales simultaneously by a factor of two. The figure reveals a clear pattern of substantially reduced scale uncertainties as the perturbative order increases. Notably, our N³LO results exhibit up to a factor of two smaller uncertainties compared to NNLO, and we anticipate further improvement once the N³LO accurate FFs become available. When compared to the experimental uncertainties from BaBar, indicated by error bars, our results demonstrate the importance of achieving N³LO accuracy to meet the precision of existing experimental data.

To quantify the impact of higher-order pQCD corrections, we further evaluate the standard K-factor, defined as the ratio of cross sections at different pQCD orders to the LO result. These K-factor, displayed as distinct colored histograms in Fig. 3, reveal increasingly significant contributions from higher order terms near the phase-space boundaries for both small- x and large- x regions. Notably, the N³LO correction can reach 30% for $x \sim 0.9$. Such a substantial correction is essential to achieve agreement with the BaBar data.

Conclusion.— In this work, we present the first analytical computation of QCD corrections to SIA at N³LO. By employing analytic continuation from DIS and explicitly evaluating the VVR and VV*R contributions, we derive

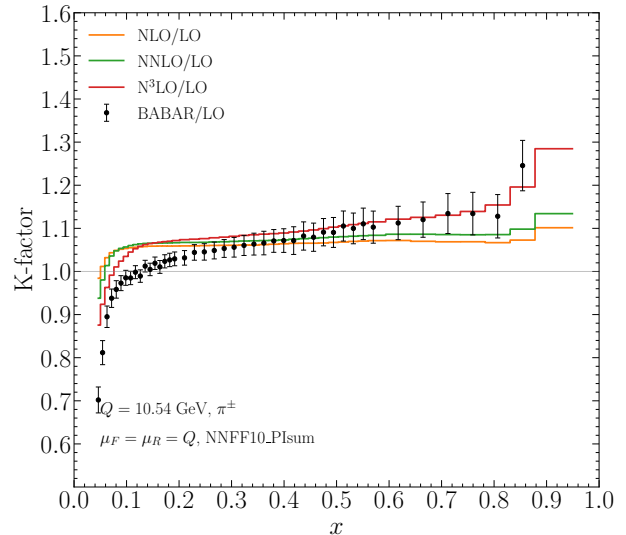


FIG. 3: The K-factor for each pQCD order, calculated with respect to the LO result, is shown by distinct colored histograms. The error bars represents the uncertainties from BaBar measurements, normalized to LO results.

the N³LO coefficient functions for the transverse and longitudinal cross sections, encapsulated in Eq. (3). Rigorous validation through pole cancellation, consistency with inclusive cross sections at N³LO, and agreement with threshold resummation at N⁴LL accuracy confirm the robustness of our results.

Phenomenologically, the N³LO predictions exhibit a marked reduction in scale uncertainties, by up to a factor of two compared to NNLO, and significantly improve the description of BaBar experimental data. The corrections are particularly pronounced in the large- x region, reaching about 30% for $x \sim 0.9$. These advancements underscore the critical role of higher-order perturbative corrections in precision QCD and provide a refined framework for extracting FFs.

Looking ahead, a global determination of N³LO FFs based on SIA data will become feasible once the full set of four-loop time-like splitting functions are available. This will further enhance the precision of hadronization studies and enable tighter constraints on non-perturbative QCD dynamics. The achieved accuracy highlights the necessity of N³LO computations in bridging the gap between theoretical predictions and experimental precision in strong interaction physics.

Acknowledgements.— We thank T. Gehrmann to provide us the Fortran package `hplog` [73]. The Feynman diagrams are drawn with the aid of `FeynGame` [74]. This work is supported by the National Science Foundation of China under Grants Nos. 12475139 and 12425505, and

by the Swiss National Science Foundation (SNF) under contract 200020-204200 and the European Research Council (ERC) under the European Union’s Horizon 2020 research and innovation programme grant agreement 101019620 (ERC Advanced Grant TOPUP).

Note added.— As we completed this work, we became aware of a related study [?], which calculates the relevant master integrals for SIA at $N^3\text{LO}$.

* legend’he@m.scnu.edu.cn

† hxing@m.scnu.edu.cn

‡ tongzhi.yang@physik.uzh.ch

§ zhuhx@pku.edu.cn

- [1] S. Navas *et al.* (Particle Data Group), *Phys. Rev. D* **110**, 030001 (2024).
- [2] S. M. Berman, J. D. Bjorken, and J. B. Kogut, *Phys. Rev. D* **4**, 3388 (1971).
- [3] R. D. Field and R. P. Feynman, *Nucl. Phys. B* **136**, 1 (1978).
- [4] J. C. Collins, D. E. Soper, and G. F. Sterman, *Adv. Ser. Direct. High Energy Phys.* **5**, 1 (1989), [arXiv:hep-ph/0409313](#).
- [5] S. Albino, *Rev. Mod. Phys.* **82**, 2489 (2010), [arXiv:0810.4255 \[hep-ph\]](#).
- [6] A. Metz and A. Vossen, *Prog. Part. Nucl. Phys.* **91**, 136 (2016), [arXiv:1607.02521 \[hep-ex\]](#).
- [7] G. Dissertori, *Adv. Ser. Direct. High Energy Phys.* **26**, 113 (2016), [arXiv:1506.05407 \[hep-ex\]](#).
- [8] P. J. Rijken and W. L. van Neerven, *Nucl. Phys. B* **487**, 233 (1997), [arXiv:hep-ph/9609377](#).
- [9] A. Mitov and S.-O. Moch, *Nucl. Phys. B* **751**, 18 (2006), [arXiv:hep-ph/0604160](#).
- [10] L. Bonino, T. Gehrmann, and G. Stagnitto, *Phys. Rev. Lett.* **132**, 251901 (2024), [arXiv:2401.16281 \[hep-ph\]](#).
- [11] S. Goyal, S.-O. Moch, V. Pathak, N. Rana, and V. Ravindran, *Phys. Rev. Lett.* **132**, 251902 (2024), [arXiv:2312.17711 \[hep-ph\]](#).
- [12] L. Bonino, T. Gehrmann, M. Löchner, K. Schönwald, and G. Stagnitto, *Phys. Rev. Lett.* **133**, 211904 (2024), [arXiv:2404.08597 \[hep-ph\]](#).
- [13] S. Goyal, R. N. Lee, S.-O. Moch, V. Pathak, N. Rana, and V. Ravindran, *Phys. Rev. Lett.* **133**, 211905 (2024), [arXiv:2404.09959 \[hep-ph\]](#).
- [14] S. Goyal, R. N. Lee, S.-O. Moch, V. Pathak, N. Rana, and V. Ravindran, (2024), [arXiv:2412.19309 \[hep-ph\]](#).
- [15] M. Czakon, T. Generet, A. Mitov, and R. Poncelet, (2025), [arXiv:2503.11489 \[hep-ph\]](#).
- [16] T. Gehrmann and G. Stagnitto, *JHEP* **10**, 136 (2022), [arXiv:2208.02650 \[hep-ph\]](#).
- [17] L. Bonino, T. Gehrmann, M. Marcoli, R. Schürmann, and G. Stagnitto, *JHEP* **08**, 073 (2024), [arXiv:2406.09925 \[hep-ph\]](#).
- [18] H. Chen, T.-Z. Yang, H. X. Zhu, and Y. J. Zhu, *Chin. Phys. C* **45**, 043101 (2021), [arXiv:2006.10534 \[hep-ph\]](#).
- [19] A. Mitov, S. Moch, and A. Vogt, *Phys. Lett. B* **638**, 61 (2006), [arXiv:hep-ph/0604053](#).
- [20] S. Moch and A. Vogt, *Phys. Lett. B* **659**, 290 (2008), [arXiv:0709.3899 \[hep-ph\]](#).
- [21] A. A. Almasy, S. Moch, and A. Vogt, *Nucl. Phys. B* **854**, 133 (2012), [arXiv:1107.2263 \[hep-ph\]](#).
- [22] V. Bertone, S. Carrazza, N. P. Hartland, E. R. Nocera, and J. Rojo (NNPDF), *Eur. Phys. J. C* **77**, 516 (2017), [arXiv:1706.07049 \[hep-ph\]](#).
- [23] D. P. Anderle, F. Ringer, and M. Stratmann, *Phys. Rev. D* **92**, 114017 (2015), [arXiv:1510.05845 \[hep-ph\]](#).
- [24] M. Soleymaninia, M. Goharipour, H. Khanpour, and H. Spiesberger, *Phys. Rev. D* **103**, 054045 (2021), [arXiv:2008.05342 \[hep-ph\]](#).
- [25] R. Abdul Khalek, V. Bertone, A. Khoudli, and E. R. Nocera (MAP (Multi-dimensional Analyses of Partonic distributions)), *Phys. Lett. B* **834**, 137456 (2022), [arXiv:2204.10331 \[hep-ph\]](#).
- [26] I. Borsa, R. Sassot, D. de Florian, M. Stratmann, and W. Vogelsang, *Phys. Rev. Lett.* **129**, 012002 (2022), [arXiv:2202.05060 \[hep-ph\]](#).
- [27] M. Li, D. P. Anderle, H. Xing, and Y. Zhao, *Phys. Rev. D* **111**, 034030 (2025), [arXiv:2404.11527 \[hep-ph\]](#).
- [28] J. Gao, X. Shen, H. Xing, Y. Zhao, and B. Zhou, (2025), [arXiv:2502.17837 \[hep-ph\]](#).
- [29] (2018), [arXiv:1809.00285 \[physics.acc-ph\]](#).
- [30] M. Dong *et al.* (CEPC Study Group), (2018), [arXiv:1811.10545 \[hep-ex\]](#).
- [31] W. Abdallah *et al.* (CEPC Study Group), *Radiat. Detect. Technol. Methods* **8**, 1 (2024), [Erratum: *Radiat. Detect. Technol. Methods* **9**, 184–192 (2025)], [arXiv:2312.14363 \[physics.acc-ph\]](#).
- [32] M. Achasov *et al.*, *Front. Phys. (Beijing)* **19**, 14701 (2024), [arXiv:2303.15790 \[hep-ex\]](#).
- [33] (2013), [arXiv:1306.6327 \[physics.acc-ph\]](#).
- [34] P. Bambade *et al.*, (2019), [arXiv:1903.01629 \[hep-ex\]](#).
- [35] A. Ayshev *et al.* (ILC International Development Team), (2022), [arXiv:2203.07622 \[physics.acc-ph\]](#).
- [36] A. Abada *et al.* (FCC), *Eur. Phys. J. C* **79**, 474 (2019).
- [37] A. Abada *et al.* (FCC), *Eur. Phys. J. ST* **228**, 261 (2019).
- [38] A. Abada *et al.* (FCC), *Eur. Phys. J. ST* **228**, 755 (2019).
- [39] P. Nason and B. R. Webber, *Nucl. Phys. B* **421**, 473 (1994), [Erratum: *Nucl. Phys. B* **480**, 755 (1996)].
- [40] B. R. Webber, in *Summer School on Hadronic Aspects of Collider Physics* (1994) pp. 49–77, [arXiv:hep-ph/9411384](#).
- [41] T. Gehrmann, E. W. N. Glover, T. Huber, N. Ikizlerli, and C. Studerus, *JHEP* **06**, 094 (2010), [arXiv:1004.3653 \[hep-ph\]](#).
- [42] S. D. Drell, D. J. Levy, and T.-M. Yan, *Phys. Rev.* **187**, 2159 (1969).
- [43] S. D. Drell, D. J. Levy, and T.-M. Yan, *Phys. Rev. D* **1**, 1035 (1970).
- [44] M.-X. Luo, T.-Z. Yang, H. X. Zhu, and Y. J. Zhu, *JHEP* **01**, 040 (2020), [arXiv:1909.13820 \[hep-ph\]](#).
- [45] J. A. M. Vermaseren, A. Vogt, and S. Moch, *Nucl. Phys. B* **724**, 3 (2005), [arXiv:hep-ph/0504242](#).
- [46] P. Nogueira, *J. Comput. Phys.* **105**, 279 (1993).
- [47] J. A. M. Vermaseren, (2000), [arXiv:math-ph/0010025](#).
- [48] B. Ruijl, T. Ueda, and J. Vermaseren, (2017), [arXiv:1707.06453 \[hep-ph\]](#).
- [49] T. van Ritbergen, A. N. Schellekens, and J. A. M. Vermaseren, *Int. J. Mod. Phys. A* **14**, 41 (1999), [arXiv:hep-ph/9802376](#).
- [50] C. Anastasiou and K. Melnikov, *Nuclear Physics B* **646**, 220 (2002).
- [51] K. G. Chetyrkin, A. L. Kataev, and F. V. Tkachov, *Nucl. Phys. B* **174**, 345 (1980).
- [52] K. G. Chetyrkin and F. V. Tkachov, *Nucl. Phys. B* **192**,

- 159 (1981).
- [53] S. Laporta, *Int. J. Mod. Phys. A* **15**, 5087 (2000), [arXiv:hep-ph/0102033](#).
 - [54] A. V. Smirnov and F. S. Chuharev, *Comput. Phys. Commun.* **247**, 106877 (2020), [arXiv:1901.07808 \[hep-ph\]](#).
 - [55] J. Klappert, F. Lange, P. Maierhöfer, and J. Usosvitsch, *Comput. Phys. Commun.* **266**, 108024 (2021), [arXiv:2008.06494 \[hep-ph\]](#).
 - [56] X. Guan, X. Liu, Y.-Q. Ma, and W.-H. Wu, *Comput. Phys. Commun.* **310**, 109538 (2025), [arXiv:2405.14621 \[hep-ph\]](#).
 - [57] T. Gehrmann and E. Remiddi, *Nucl. Phys. B* **580**, 485 (2000), [arXiv:hep-ph/9912329](#).
 - [58] V. Magerya and A. Pikelner, *JHEP* **12**, 026 (2019), [arXiv:1910.07522 \[hep-ph\]](#).
 - [59] V. Maheria, *Semi- and Fully-Inclusive Phase-Space Integrals at Four Loops*, Ph.D. thesis, Hamburg U. (2022).
 - [60] R. N. Lee, (2012), [arXiv:1212.2685 \[hep-ph\]](#).
 - [61] J. M. Henn, *Phys. Rev. Lett.* **110**, 251601 (2013), [arXiv:1304.1806 \[hep-th\]](#).
 - [62] C. Meyer, *Comput. Phys. Commun.* **222**, 295 (2018), [arXiv:1705.06252 \[hep-ph\]](#).
 - [63] E. Remiddi and J. A. M. Vermaseren, *Int. J. Mod. Phys. A* **15**, 725 (2000), [arXiv:hep-ph/9905237](#).
 - [64] D. Maitre, *Comput. Phys. Commun.* **174**, 222 (2006), [arXiv:hep-ph/0507152](#).
 - [65] C. Duhr and F. Dulat, *JHEP* **08**, 135 (2019), [arXiv:1904.07279 \[hep-th\]](#).
 - [66] S. Moch, J. A. M. Vermaseren, and A. Vogt, *Nucl. Phys. B* **688**, 101 (2004), [arXiv:hep-ph/0403192](#).
 - [67] A. Vogt, S. Moch, and J. A. M. Vermaseren, *Nucl. Phys. B* **691**, 129 (2004), [arXiv:hep-ph/0404111](#).
 - [68] S. Gorishny, A. Kataev, and S. Larin, *Physics Letters B* **259**, 144 (1991).
 - [69] L. R. Surguladze and M. A. Samuel, *Phys. Rev. Lett.* **66**, 560 (1991).
 - [70] Z. Xu and H. X. Zhu, (2024), [arXiv:2411.11595 \[hep-ph\]](#).
 - [71] P. Jakubčík, M. Marcoli, and G. Stagnitto, *JHEP* **01**, 168 (2023), [arXiv:2211.08446 \[hep-ph\]](#).
 - [72] J. P. Lees *et al.* (BaBar), *Phys. Rev. D* **88**, 032011 (2013), [arXiv:1306.2895 \[hep-ex\]](#).
 - [73] T. Gehrmann and E. Remiddi, *Comput. Phys. Commun.* **141**, 296 (2001), [arXiv:hep-ph/0107173](#).
 - [74] L. Bündgen, R. V. Harlander, S. Y. Klein, and M. C. Schaaf, (2025), [arXiv:2501.04651 \[hep-ph\]](#).
 - [75] V. Magerya and L. Fekésházy, (2025), [arXiv:2503.19837 \[hep-ph\]](#).